MATERIALS CHEMISTRY FRONTIERS

RESEARCH ARTICLE

View Article Online
View Journal | View Issue

Cite this: *Mater. Chem. Front.*, 2021, **5**, 1863

Facile construction of well-defined radical metallacycles through coordination-driven self-assembly†

Qian Tu,[a] Gui-Fei Huo,[a] Xiao-Li Zhao,[a] Haitao Sun,[b] Xueliang Shi*[a] and Hai-Bo Yang*[a]

Recently, the marriage of organic radicals and supramolecular chemistry has given birth to a booming research field of supramolecular radical chemistry. However, the well-developed supramolecular radical systems are still limited, especially at present the supramolecular coordination radical systems are rarely explored. The construction of discrete supramolecular radical coordination complexes such as radical metallacycles and metallacages still remains a great challenge mainly because of the intrinsically unstable nature of organic radicals and the lack of suitable coordination method. Herein, we design and synthesize a new organic radical ligand **CzBTM-Py** with well-defined coordination geometry and persistent stability. Subsequently, two discrete radical metallacycles of **M1** and **M2** are successfully and efficiently constructed *via* the coordination-driven self-assembly approach. Due to the mild coordination reaction conditions the open-shell nature of **CzBTM-Py** is preserved as indicated by the electron paramagnetic resonance (EPR) spectroscopy. The chemical structures of **CzBTM-Py**, **M1** and **M2** are successfully determined by X-ray crystallography. Interestingly, a chiral self-sorting behavior is observed in this coordination-driven self-assembly process, *i.e.*, **M1** exists as *MM*/*PP* enantiomers couple while **M2** exists as the heterochiral *PM* form. Moreover, the photophysical properties of the radicals have changed significantly after coordination, making the color and emission of **M1** and **M2** differ from those of **CzBTM-Py**. Additionally, metallacycles **M1** and **M2** show better photostability than radical ligand **CzBTM-Py**. This work successfully demonstrates a highly efficient coordination-driven self-assembly approach to synthesize radical-based supramolecular coordination complexes, which could modulate the chemical and physical properties of organic radicals, and thus to develop new functional metal–organic radical materials.

Received 27th November 2020,
Accepted 8th January 2021

DOI: 10.1039/d0qm00992j

rsc.li/frontiers-materials

Introduction

Free radicals are compounds that feature unpaired electrons or open-shell electronic configurations. Since the landmark discovery of the persistent organic radicals by Moses Gomberg in 1900,[1] the design and synthesis of stable organic radicals has been very attractive but also great challenge to chemists.[2] Most organic radicals are highly reactive and readily undergo dimerization, hydrogen abstraction, disproportionation and other reactions, therefore usually unstable.[3,4] Due to their distinct open-shell nature and special reactivity, organic radicals have played increasingly important roles in the field of organic synthesis, biology, and functional materials.[5,6] For example, organic radicals are involved in many synthetic transformations and have been widely used as (co)catalysts for the oxidation, mediators for living radical polymerization, and antioxidants.[7–9] Organic free radicals are actually produced continuously in biosystems and play an important role in a number of biological processes, *e.g.*, efficiently transforming air and food into chemical energy in the human body largely depends on the chain reactions of free radicals.[10] Organic radicals with intrinsic magnetic nature have also demonstrated the wide application in the field of spin trapping, spin labelling, EPR imaging, and dynamic nuclear polarization (DNP).[11–14] Moreover, organic radicals have been intensively employed as functional building blocks to construct a variety of radical-based functional materials such as organic magnetic materials, organic spintronics, organic conductors, organic radical batteries, and so on.[15,16] Particularly, organic radicals are recently emerging as peculiar luminescent materials and have demonstrated great

[a] *Shanghai Key Laboratory of Green Chemistry and Chemical Processes, School of Chemistry and Molecular Engineering, East China Normal University, Shanghai 200062, P. R. China. E-mail: xlshi@chem.ecnu.edu.cn, hbyang@chem.ecnu.edu.cn*
[b] *State Key Laboratory of Precision Spectroscopy, School of Physics and Electronic Science, East China Normal University, Shanghai, 200241, P. R. China*

† Electronic supplementary information (ESI) available. CCDC 2045293 (**CzBTM-Py**), 2045295 (**M1**) and 2045294 (**M2**). For ESI and crystallographic data in CIF or other electronic format see DOI: 10.1039/d0qm00992j

success in the application of highly efficient radical-based organic light-emitting diodes (OLEDs).[17–22] Notably, organic radicals have also aroused extensive attention in the field of supramolecular chemistry, leading to a booming research field of supramolecular radical chemistry.[23–25] The most pioneer work in this field is the study of the various organic radical cation dimerization and their host–guest chemistry and self-assembly.[26–30] However, the supramolecular radical systems reported so far are still limited to radical cation-based host–guest systems, while the supramolecular coordination radical systems are still less explored.[31–37]

The marriage of organic radical chemistry and coordination chemistry, namely radical coordination chemistry, could potentially spark some new design ideas and eventually create new radical-based molecules and materials.[38] It has demonstrated that the coordination of organic radicals has a profound effect on the properties of the resultant radical complexes such as the ligand radical reactivity and their magnetic exchange coupling, which are very important to implement their practical applications in organic synthesis and magnetic properties. Specifically, organic radicals can react with transition-metal complexes in many different ways accompanied by various valuable organic reactions and important biological processes.[38] Organic radicals, as unique bridging ligands, could efficiently facilitate strong magnetic exchange coupling between high-anisotropy paramagnetic metal centers, which represents a classical rule to design high temperature single-molecule magnets.[39–41] Moreover, recent reports have also demonstrated that the coordination of the luminescent radicals to gold(I) could affect the electronic states of radicals and significantly enhance their fluorescence quantum yield and photostability.[42,43] To date, a wide variety of metal-radical coordination complexes ranging from simple radical-molecule complexes to infinite one-dimensional coordination chains and two- and three-dimensional metal-radical networks have been successfully constructed.[41,44] However, to the best of our knowledge, discrete radical metallacycles are rarely reported and documented, probably due to the challenging design and synthesis of the suitable radical ligands with well-defined coordination geometry and persistent stability.[37,45,46] Moreover, the novel mild and efficient coordination method is also highly anticipated to prepare discrete radical metallacycles.

Coordination-driven self-assembly has proven to be a powerful approach to construct a diverse range of supramolecular coordination complexes with well-controlled shapes and sizes, including metallacycles, metallacages, and metal–organic frameworks (MOFs), through the combination of a range of diverse functional ligands and complementary metal salts.[47–61] The employment of coordination-driven self-assembly methodology to construct discrete radical metallacycles (Fig. 1) is expected to show several distinct merits including: (1) the coordination-driven supramolecular self-assembly reaction conditions are very mild without adding any acid/base or catalyst; (2) the coordination-driven self-assembly approach is very efficient with no need for the tedious purification steps; (3) the combination of different organometallic acceptors with organic radical ligand could result in a diverse library of metal–organic coordination complexes with different conformations; and (4) the introduction of heavy atoms like Pt may lead to some interesting photophysical properties of organic radicals. In addition to the coordination method, the rational design of the suitable ditopic or polytopic organic radical ligands with well-defined coordination geometry and persistent stability is also crucially important because radical ligands not only dictate the structure and topology of the resulting radical-based supramolecular architectures but also determine their properties and applications.

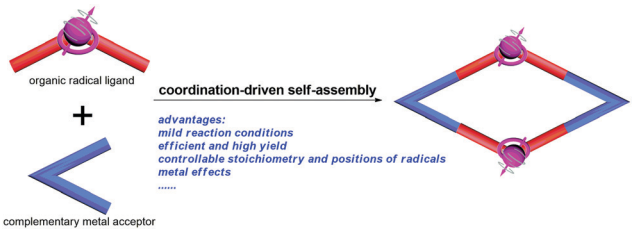

Fig. 1 Cartoon representation of the construction of discrete radical metallacycle through the coordination-driven self-assembly approach in this work and its advantages.

In this work, we design and synthesize a new dipyridyl-functionalized (*N*-carbazolyl)bis(2,4,6-trichlorophenyl) methyl radical (**CzBTM-Py**) which serves as a stable ligand with conformational rigidity and well-defined coordinate vectors. Subsequently, efficient coordination-driven self-assembly of the radical ligand **CzBTM-Py** with the complementary metal acceptors resulted in two well-defined radical metallacycles, namely **M1** and **M2**. Notably, continuous wave electron paramagnetic resonance (CW-EPR) spectroscopy revealed that the open-shell nature of radical ligand **CzBTM-Py** was preserved in the resultant metallacycles, mainly because of the relatively long persistence of radical **CzBTM-Py** and the mild reaction conditions in such coordination-driven self-assembly process. The crystal structure of **CzBTM-Py** is determined by single crystal X-ray diffraction and shows that **CzBTM-Py** exists in two different enantiomeric forms of *P* and *M*. Interestingly, metallacycles **M1** and **M2** displayed distinct well-defined shapes and sizes as well as intriguing chiral self-sorting behavior as indicated in their single crystals. With regard to their photophysical properties, the radical ligand **CzBTM-Py** and metallacycles **M1** and **M2** differ in their color and emission. Moreover, the radical stability studies revealed that metallacycles **M1** and **M2** showed better photostability than those of radical ligand **CzBTM-Py**. Therefore, this study demonstrates that coordination-driven self-assembly is a facile and versatile strategy for the preparation of discrete radical supramolecular coordination complexes. The preliminary results in this work also successfully prove the importance of supramolecular coordination approach in modulation of the chemical and physical properties of organic radicals, which may open up a new avenue to develop functional metal–organic radical materials.

Results and discussion

Synthesis and characterization of the radical ligand CzBTM-Py

Polychlorotriphenylmethyl radicals such as perchlorotriphenyl methyl (PTM) and tris(2,4,6-trichlorophenyl)methyl (TTM) radicals

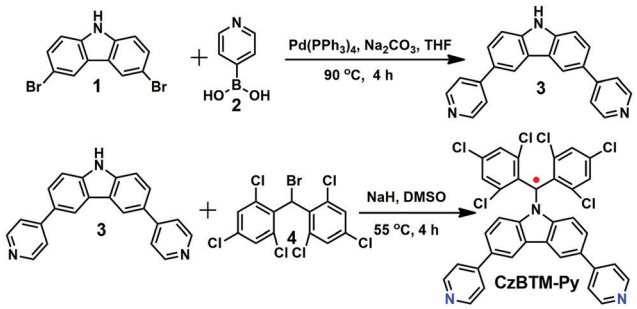

Scheme 1 Synthetic route to **CzBTM-Py**.

are reported to be very stable and easily chemically modified. Thus, a new ditopic TTM-based radical ligand, namely **CzBTM-Py** bearing two 4-pyridyl groups, was designed in this work. **CzBTM-Py** was successfully synthesized by a two-step procedure as illustrated in Scheme 1. First, a Suzuki coupling reaction of 3,6-dibromocarbazole **1** with 4-pyridinylboronic acid **2** afforded 3,6-di(4-pyridyl) carbazole **3** in 41% yield. Subsequently, a nucleophilic substitution reaction of **3** with (bromomethylene)bis(2,4,6-trichlorobenzene) **4** accompanying a DMSO-mediated oxidation resulted in **CzBTM-Py** in moderate yield (24%).[62] Notably, **CzBTM-Py** is very stable and could be purified by column chromatography. Due to the paramagnetic nature, the proton nuclear magnetic resonance (^{1}H NMR) spectrum of **CzBTM-Py** experienced seriously signal broadening (see the ESI,† Fig. S12), leading to very difficult to identify its exact structure. Nevertheless, the structure of **CzBTM-Py** was unambiguously confirmed by electrospray ionization mass spectrometry (ESI-MS) (Fig. S19, ESI†) and X-ray crystallographic analysis (*vide infra*). The single crystal of **CzBTM-Py** further confirmed its good conformational rigidity and well-defined coordinate vectors that is readily able to coordinate with suitable di-Pt(II) acceptors.

Self-assembly of radical metallacycles M1 and M2 and their characterization

Since **CzBTM-Py** is a nearly 90° dipyridyl acceptor, two complementary metal acceptors of **A1** and **A2** are elaborately chosen to construct two metallacycles with different shapes and sizes.[63,64] As shown in Scheme 2, metallacycle **M1** with PF_6^- counterion was prepared by simply mixing the radical ligand **CzBTM-Py** with the 90° diplatinum(II) acceptor **A1** in 1 : 1 ratio in a mixed solvent of acetone and water at 50 °C, and then adding a saturated aqueous solution of KPF_6 to precipitate the dark red products with high yield up to 90%. Similarly, metallacycle **M2** with OTf^- (OTf^- = trifluoromethanesulfonate) counterion was prepared in high yield (~90%) *via* coordination-driven self-assembly from **CzBTM-Py** and corresponding acceptor of **A2** in CH_2Cl_2 at room temperature. It is also worth noting that the open-shell nature of **CzBTM-Py** is preserved in the resultant metallacycles **M1** and **M2**, mainly because of the relatively long persistence of radical **CzBTM-Py** and the mild reaction conditions in such coordination-driven self-assembly process. Consequently, the signal peak broadening was also significant in the ^{1}H NMR

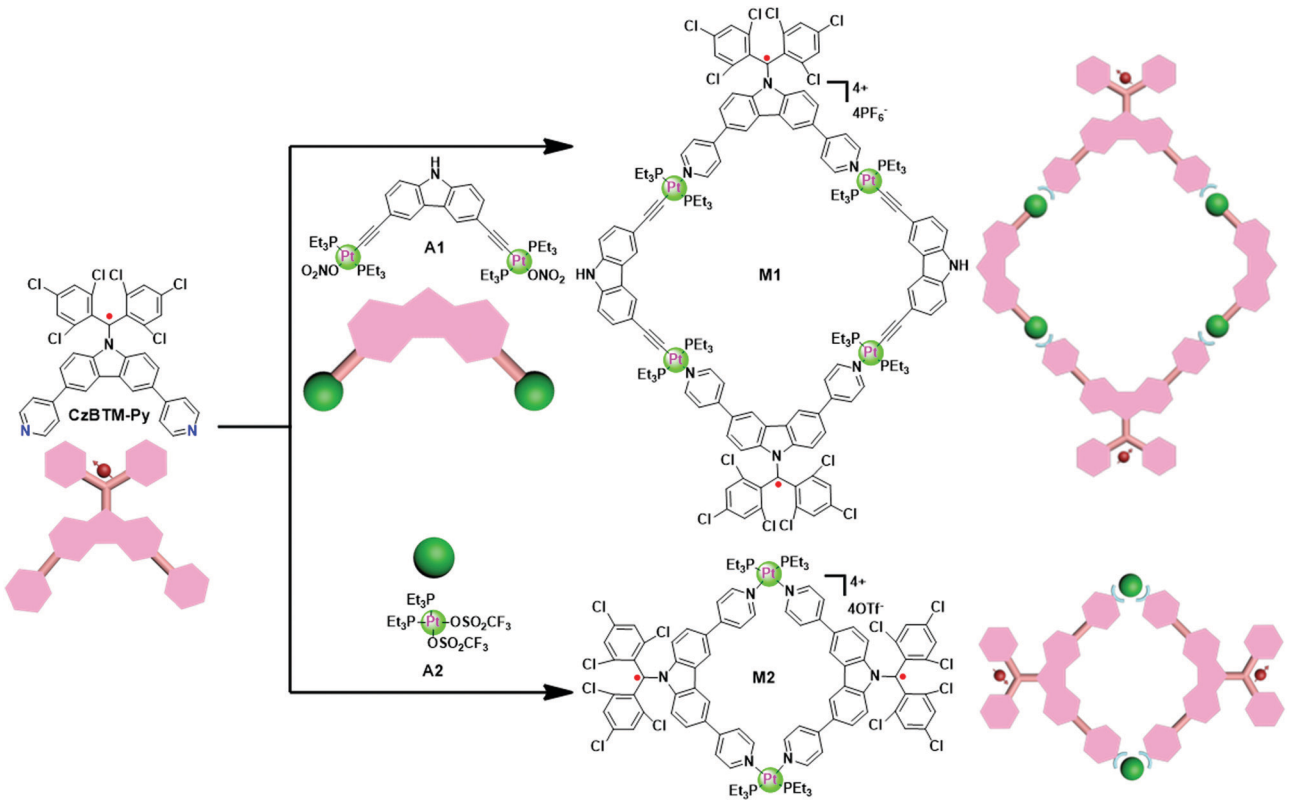

Scheme 2 Self-assembly of metallacycles **M1** and **M2**.

spectra of **M1** and **M2**, making it difficult to characterize their structure by conventional NMR spectroscopy (Fig. S14–S17, ESI†). Nevertheless, the ESI-MS-TOF mass spectrometry provided further evidence for the formation of the target of **M1** and **M2** (Fig. S20 and S21, ESI†). Specifically, the observed peaks for **M1** and **M2** were all isotopically resolved and agreed well with their corresponding simulated isotope pattern, supporting the formation of a discrete structure as the sole assembly product. Finally, the absolute structures of **M1** and **M2** were successfully determined by X-ray crystallographic analysis (*vide infra*).

CW-EPR spectroscopy studies

CW-EPR is then employed to characterize the radical signature of **CzBTM-Py**, **M1** and **M2**. As shown in Fig. 2a, solution-state CW-EPR spectra of **CzBTM-Py**, **M1** and **M2** all revealed a dominant sharp peak with $g \approx 2.003$, illustrating the existence of the unpaired electron in their structures. The sharp peak was accompanied by very weak satellite lines, which were attributed to the natural abundant ^{13}C hyperfine coupling. The hyperfine coupling with ^{1}H or ^{14}N was hardly observed, implying that the spin density is mainly distributed on the central trivalent C atom. Similarly, solid-state EPR spectra of **CzBTM-Py**, **M1** and **M2** also showed a single peak, while the peak became significantly broadened due to their dipole–dipole interactions in the solid state (Fig. 2b). No forbidden half-field transition was observed in the EPR spectra of **M1** and **M2** despite of their potential biradical nature in the ground state. The absence of the forbidden half-field transition implies the very week spin–spin interactions in **M1** and **M2**, mainly attributed to the very long distance between the two radicals in **M1** and **M2**, which do not favor the spin–spin interaction.[65]

X-ray crystallographic analysis

X-ray-quality single crystal of radical ligand **CzBTM-Py** was easily grown by slow diffusion of methanol into chloroform solution at room temperature. As shown in Fig. 3a, the crystal structure of **CzBTM-Py** consists of a trivalent, sp^2-hybridized carbon atom that is connected to three sterically hindered aromatic rings, implying its open-shell nature. The bulky chlorine atoms caused the two 2,4,6-trichlorophenyl groups to have a highly twist orientation, *i.e.*, the torsion angles between the plane of carbazole group and the plane of trichlorophenyl group were determined to be approximately

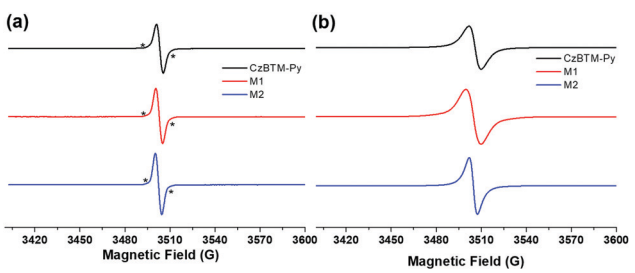

Fig. 2 Room-temperature CW X-band EPR spectra of **CzBTM-Py**, **M1** and **M2** in the solution state (a) and solid state (b). * indicates ^{13}C hyperfine coupling.

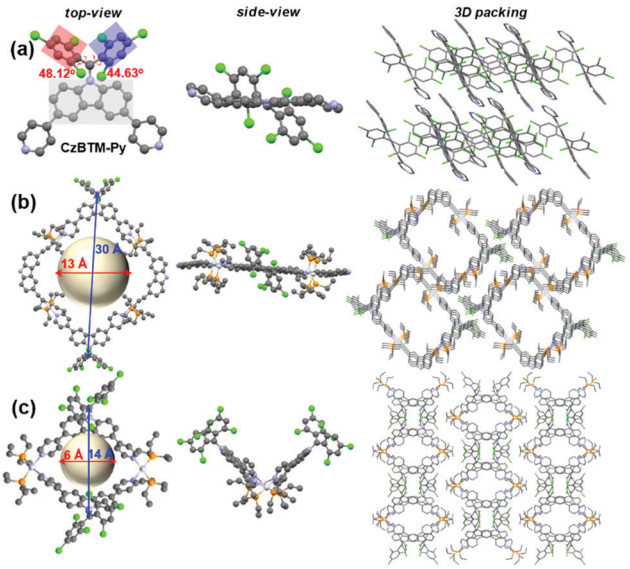

Fig. 3 ORTEP drawings and 3D packing structures of (a) **CzBTM-Py**, (b) **M1**, and (c) **M2**. Hydrogen atoms, anions and solvent are omitted for clarity.

48.12° and 44.63° (Fig. 3a). **CzBTM-Py** crystalized in layers with strong intermolecular π–π stacking interaction (Fig. 3a). Single crystals of metallacycles **M1** and **M2** were also grown by slow diffusion of isopropyl ether into dichloromethane solution at the room temperature. After coordination, the structural integrity of **CzBTM-Py** is maintained in **M1** and **M2**, further implied that the radical is persistent under this mild self-assembly reaction condition. In their crystal forms, metallacycle **M1** was nearly square and planar, while metallacycle **M2** exhibited a bowl shape as indicated from the side view (Fig. 3b and c). The non-planar conformation of **M2** is mainly due to the reversible thermodynamic nature of the coordination-driven self-assembly process wherein **CzBTM-Py** and **A2** are prone to adopt the most comfortable coordination geometry and form the thermodynamically stable [2+2] metallacycle **M2**. The diameters of the internal cavity of **M1** and **M2** were determined to be approximately 13 Å and 6 Å, respectively. Notably, the spin–spin distances between the two radicals in **M1** and **M2** were around 30 Å and 14 Å, respectively. Such ultra-long distance could account for the weak spin–spin interactions in **M1** and **M2** as revealed by their single-line EPR spectra.[65] The metallacycles **M1** and **M2** further packed into columns with well-defined channel size. No obvious intermolecular stacking interaction was existed between the radical centers, implying the weak intermolecular spin–spin interactions in **M1** and **M2**. To the best of our knowledge, this represents one of very few examples of the discrete radical metallacycles being characterized by X-ray crystallography.

Chiral self-sorting behavior

Polychlorotriphenylmethyl radicals and their derivatives are intrinsically chiral because of their propeller-like conformation with a considerable rotational energy barrier.[66] As a result, these radicals have two atropisomeric forms of *Plus* (*P*) and *Minus* (*M*) according to the Cahn–Ingold–Prelog (CIP) nomenclature.[67]

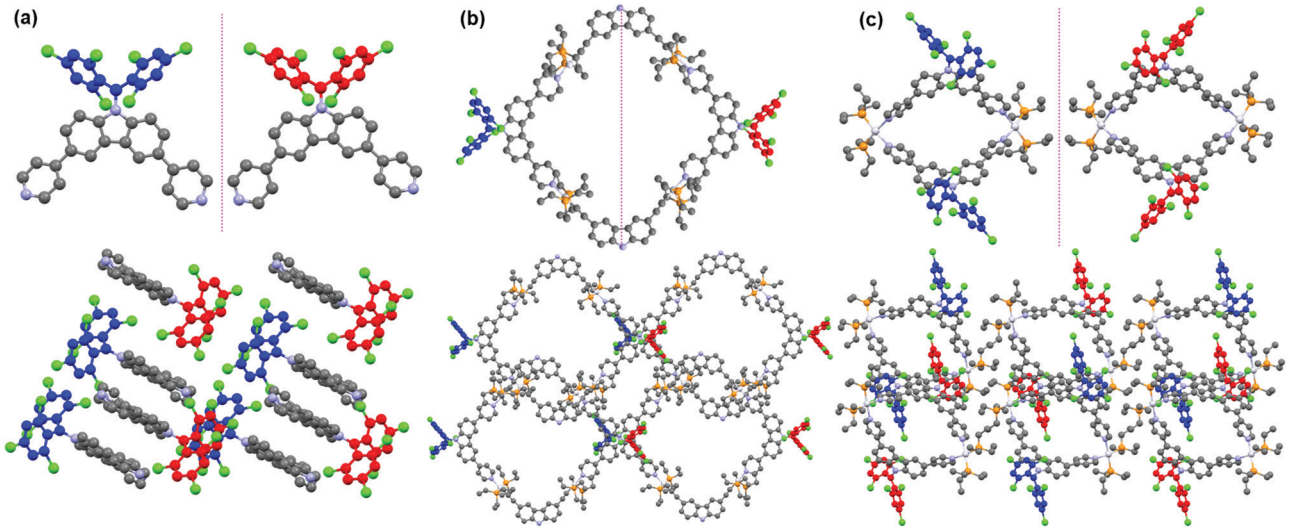

Fig. 4 (a) *M* (blue) and *P* (red) enantiomer of **CzBTM-Py**. Chiral self-sorting behavior of metallacycles **M1** (b) and **M2** (c).

Similarly, radical ligand **CzBTM-Py** also exists in two different enantiomeric forms *M* (blue) and *P* (red) as indicated in its single crystal (Fig. 4a). The energy barrier of **CzBTM-Py** was calculated to be ~23.23 kcal mol^{-1} (Fig. S27, ESI†), which also agree well with the literature.[66] Upon self-assembly with the complementary metal acceptors, several possible stereoisomers are expected in the resultant [2+2] metallacycles **M1** and **M2**, including the homochiral assemblies of *MM* and *PP*, and the heterochiral assembly of *PM*. Interestingly, metallacycle **M1** is heterochiral assembly consisting of a *M*-enantiomer and a *P*-enantiomer of **CzBTM-Py**, while no homochiral assemblies of *MM* or *PP* enantiomer is observed in this process (Fig. 4b). In comparison, self-assembly of two **CzBTM-Py** units with **A2** results in only the *MM*/*PP* enantiomers couple of metallacycle **M2** (Fig. 4c), whereas the heterochiral assembly of *PM* is not observed in this coordination-driven self-assembly process. Therefore, these results imply the distinct chiral self-sorting behavior of the metallacycles **M1** and **M2** along their self-assembly process. The underlying mechanism of such chiral self-sorting behavior is not clear and might be related to the reversible thermodynamic nature of the coordination-driven self-assembly process in which the final coordination species tend to form the thermodynamically preferred discrete supramolecular entities in their single crystals.[68] Notably, the two enantiomers of **CzBTM-Py** and **M2** are difficult to separate because of their relatively small energy barrier at room temperature, and also the lack of the suitable chiral stationary phase (CSP) columns.[69]

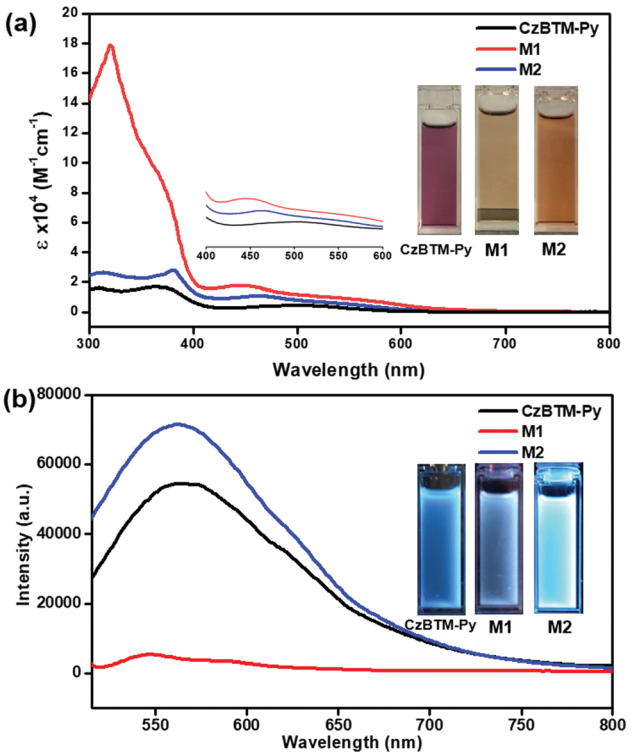

Fig. 5 (a) UV-Vis absorption spectra of 10 μM **CzBTM-Py**, **M1** and **M2** in CH_2Cl_2 solution; (b) emission spectra of **CzBTM-Py** (10 μM), **M1** (5 μM) and **M2** (5 μM) in CH_2Cl_2 solution (λ_{ex} = 490 nm); insert are the photos of their solutions under daylight (a) and UV light (365 nm) (b).

Photophysical properties

Very recently, polychlorotriphenylmethyl radicals and their derivatives have demonstrated to exhibit peculiar luminescent feature, which is very important to improve the efficiency of conventional OLED.[17–22] Thus, the photophysical properties of **CzBTM-Py**, **M1** and **M2** have been surveyed in this study. As shown in Fig. 5a, **CzBTM-Py** featured two relatively strong absorption peaks between 300 nm and 400 nm and a very weak broad absorption band extending from *ca.* 420 nm into *ca.* 650 nm. The resultant broad absorption band can be assigned to the characteristic absorption of carbon-centered radicals. After coordination, metallacycle **M2** experienced a very similar absorption profile to that of **CzBTM-Py**, while metallacycle **M1** exhibited strong absorption under 400 nm. The strong absorption peak at 320 nm is very likely caused by the acceptor

ligand of **A1** which contains carbazole moiety since the later one showed absorption peak in this region (Fig. S22, ESI†). Notably, the molar absorption coefficient of metallacycles **M1** and **M2** is significantly enhanced compared with that of radical ligand **CzBTM-Py** largely because the metallacycles contain two **CzBTM-Py** chromophores (Fig. S23, ESI†). As a consequence, the solution of **CzBTM-Py** is somewhat red while the color of metallacycles **M1** and **M2** is yellow brown. With regard to their emission properties (Fig. 5b), **CzBTM-Py** is very weak luminescent in contrast to its precursor analogue **CzBTM** featuring strong emission.[62] The weak emissive property of **CzBTM-Py** might be attributed to the potential enhanced intersystem crossing induced by the 4-pyridyl substituent, thus quenching the ligand fluorescence.[70] The preliminary results also revealed that the supramolecular coordination seemed to have an effect on the luminescent properties of radicals, *e.g.*, coordination-driven self-assembly process decreased the fluorescence intensity of metallacycle **M1** while increased the fluorescence intensity of **M2**. Notably, the fluorescence quantum yield (Φ) of **CzBTM-Py**, **M1** and **M2** was extremely low and the exact Φ value was virtually impossible to probe by the relative method (Fig. S24, ESI†). Interestingly, **CzBTM-Py**, **M1** and **M2** displayed very weak blue emission in dark upon UV-light irradiation (365 nm), which is mainly derived from the carbazole chromophore (Fig. 5b). The underlying mechanism of the coordination effect on the emissive properties of radicals is unknown and might be related to the metal-to-ligand charge transfer (MLCT) or ligand-to-metal charge transfer (LMCT),[71] and the related investigation is in progress in our laboratory.

Stability studies

Polychlorotriphenylmethyl radicals are reported to be persistent and stable to air and moisture, and can be kept for a long period in the absence of light.[66] As shown in Fig. 6a and Fig. S2–S4 (ESI†), the EPR intensity of the solution of **CzBTM-Py**, **M1** and **M2** was measured over 1000 min in the dark condition. The results revealed that **CzBTM-Py**, **M1** and **M2** were very stable even after long-term storage under ambient condition, which is consistent with the literature. However, upon irradiation (200 to 2000 nm) **CzBTM-Py** was thoroughly decomposed within 5 min, while a much longer time (~20 min) was needed for **M2** to be completely degraded (Fig. 6a and Fig. S5–S8, ESI†). Notably, metallacycle **M1** had a higher resistance to light compared to **CzBTM-Py** and **M2**, *e.g.*, **M1** still kept about 30% while the other two were totally decomposed under this irradiation condition. The enhancement of the photostability of metallacycles was probably due to their rigid and tightly packed architectures, which decreases its exposed molecular surface area and protects it from oxygen and moisture under light condition. In addition, **CzBTM-Py**, **M1** and **M2** could be heated up to 250 °C as confirmed from their thermogravimetric analysis (TGA), indicating their good thermal stability (Fig. S9, ESI†).

Experimental

Compound **4** and metal acceptors of **A1** and **A2** were prepared according to the literature.[62–64,72]

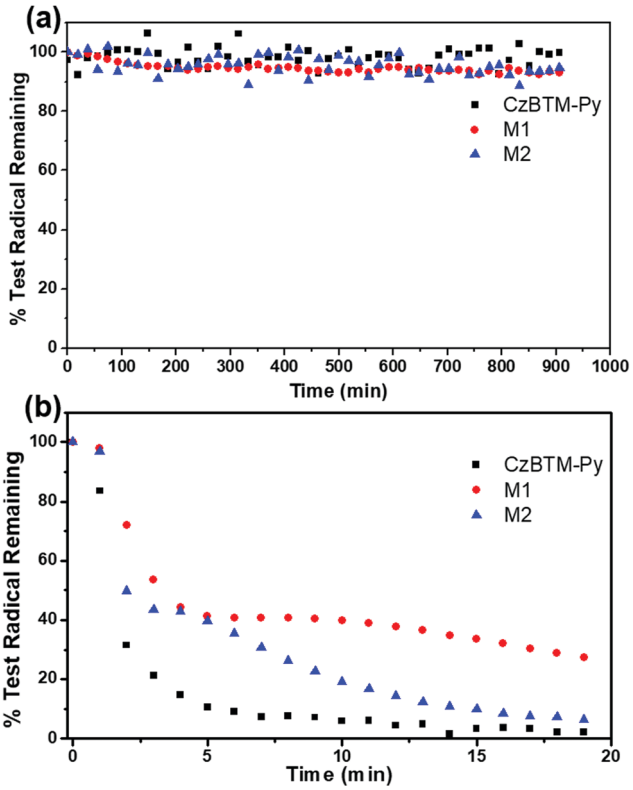

Fig. 6 EPR signal fading of **CzBTM-Py**, **M1** and **M2** in the dark condition (a) and upon irradiation (b).

Synthesis of 3

A degassed solution of the 3,6-dibromocarbazole **1** (5.0 g, 15.0 mmol) in THF/H_2O (4 : 1, 200 mL) were added 4-pyridinylboronic acid **2** (11.4 g, 90.0 mmol), $Pd(PPh_3)_4$ (1.8 g, 1.5 mmol) and Na_2CO_3 (6.5 g, 61.0 mmol). The resultant solution was stirred at 80 °C for 48 h under an inert atmosphere. The solvent was then removed by evaporation on a rotary evaporator. The residue was purified by column chromatography on silica gel (dichloromethane/acetone = 1 : 1, two drops of NEt_3) to get the product **3** as a pale-yellow solid (2.4 g, 50% yield). ^{1}H NMR (500 MHz, DMSO-d_6, ppm): δ 11.67 (s, 1H), 8.83 (s, 2H), 8.64 (d, J = 5.4 Hz, 4H), 7.91 (d, J = 8.5 Hz, 2H), 7.85 (d, J = 5.5 Hz, 4H), 7.64 (d, J = 8.5 Hz, 2H). ^{13}C NMR (126 MHz, DMSO-d_6) δ 150.23, 147.95, 141.01, 127.97, 124.93, 123.46, 121.01, 119.39, 111.99. HR-EI-MS: m/z calculated for $C_{22}H_{15}N_3$ $[M]^+$: 321.1266, found: 321.1270.

Synthesis of CzBTM-Py

Under N_2 atmosphere, sodium hydride (60% in oil, 58.7 mg, 1.5 mmol) was dispersed in a solution of anhydrous dimethyl sulfoxide (20 mL), compound **3** (500.0 mg, 1.6 mmol) dissolved in anhydrous dimethyl sulfoxide (5 mL) was added dropwise and stirred until that no gas was generated. Compound **4** (458.3 mg, 1.0 mmol) was added into the mixture and stirred for 3 h under 55 °C. Next, the mixture was cooled to room temperature and saturated ammonium chloride solution (50 mL) was added slowly. The precipitate was collected by

suction filtration and purified by flash column chromatography (silica gel, dichloromethane/petroleum ether = 1 : 8), after that, preparative thin layer chromatography (PTLC) was carried out to get the pure product as a dark red solid (150.0 mg, 24% yield). ^{1}H NMR and ^{13}C NMR of **CzBTM-Py** are not detected owing to its strong paramagnetic broadening. HR-ESI-MS: *m*/*z* calculated for $C_{35}H_{18}Cl_6N_3$ $[M + H]^+$: 692.9602, found: 692.9672.

Self-assembly of metallacycle M1

CzBTM-Py (20.0 mg, 28.8 μmol) and diplatinum(II) acceptor **A1** (34.6 mg, 28.8 μmol) were weighed accurately into a glass vial, and then added 5.0 mL acetone and 1.0 mL water. The reaction solution was then stirred at 55 °C in dark overnight to yield a homogeneous fuchsia solution. Then the saturated KPF_6 solution was added into the bottle with continuous stirring (5 min) to precipitate the product. The reaction mixture was centrifuged, washed several times with water, and dried by freeze-dryer. The product **M1** was obtained as a dark red solid (53.4 mg, 90% yield).

Self-assembly of metallacycle M2

CzBTM-Py (10.0 mg, 14.4 μmol) and organoplatinum acceptor **A2** (10.5 mg, 14.4 μmol) were weighed accurately into a glass vial, and then added 2.0 mL CH_2Cl_2. The reaction solution was then stirred at room temperature in the dark for 12 hours. After removing most of the solvent, some drops of ether was added to precipitate the product. The reaction mixture was then centrifuged, washed several times with ether. Dark red powder **M2** was gained in 90% yield (18.4 mg) after drying the residue.

Conclusions

In summary, we have designed and synthesized a new ditopic radical ligand **CzBTM-Py** bearing two 4-pyridyl groups, which has persistent stability and well-defined coordination geometry that is readily able to coordinate with suitable di-Pt(II) acceptors. Two well-defined radical metallacycles **M1** and **M2** were then successfully constructed *via* the coordination-driven self-assembly approach. The structures of **CzBTM-Py**, **M1** and **M2** were unambiguously determined by mass spectrometry and X-ray crystallography. Metallacycle **M1** was nearly square and planar while metallacycle **M2** exhibited a bowl shape in the solid state, illustrating the metal ligand effect on the geometry of assemblies. Intriguingly, a distinct chiral self-sorting behavior of the metallacycles **M1** and **M2** was also observed in their single crystals. Moreover, this study also proves that the supramolecular coordination approach could affect the photophysical properties and stabilities of **CzBTM-Py**. Therefore, this work has demonstrated the power of coordination-driven self-assembly approach to construct radical-based supramolecular coordination complexes which may serve as functional metal–organic radical materials in the future.

Conflicts of interest

There are no conflicts to declare.

Acknowledgements

H.-B. Y. thanks Innovation Program of Shanghai Municipal Education Commission (No. 2019-01-07-00-05-E00012), Program for Changjiang Scholars and Innovative Research Team in University for financial support. X. S. acknowledges the financial supports sponsored by NSFC/China (No. 22071061), Shanghai Sailing Program (19YF1412900), and the Fundamental Research Funds for the Central Universities. We thank the staffs from BL17B beamline of National Facility for Protein Science in Shanghai (NFPS) at Shanghai Synchrotron Radiation Facility, for assistance during data collection.

Notes and references

1 M. Gomberg, An instance of trivalent carbon: triphenylmethyl, *J. Am. Chem. Soc.*, 1900, **22**, 757–771.
2 R. G. Hicks, What's new in stable radical chemistry?, *Org. Biomol. Chem.*, 2007, **5**, 1321–1338.
3 K. Kato and A. Osuka, Platforms for Stable Carbon-Centered Radicals, *Angew. Chem., Int. Ed.*, 2019, **58**, 8978–8986.
4 Z. Zeng, X. Shi, C. Chi, J. T. López Navarrete, J. Casado and J. Wu, Pro-aromatic and anti-aromatic π-conjugated molecules: an irresistible wish to be diradicals, *Chem. Soc. Rev.*, 2015, **44**, 6578–6596.
5 I. Ratera and J. Veciana, Playing with organic radicals as building blocks for functional molecular materials, *Chem. Soc. Rev.*, 2012, **41**, 303–349.
6 M. Abe, Diradicals, *Chem. Rev.*, 2013, **113**, 7011–7088.
7 S. Mukherjee and B. List, Radical catalysis, *Nature*, 2007, **447**, 152–153.
8 D. Leifert and A. Studer, The Persistent Radical Effect in Organic Synthesis, *Angew. Chem., Int. Ed.*, 2020, **59**, 74–108.
9 M. Yan, J. C. Lo, J. T. Edwards and P. S. Baran, Radicals: Reactive Intermediates with Translational Potential, *J. Am. Chem. Soc.*, 2016, **138**, 12692–12714.
10 O. I. Aruoma, Nutrition and health aspects of free radicals and antioxidants, *Food Chem. Toxicol.*, 1994, **32**, 671–683.
11 E. G. Janzen and Spin Trapping, *Acc. Chem. Res.*, 1971, **4**, 31–40.
12 M. R. Fleissnera, E. M. Brustad, T. Kalaic, C. Altenbacha, D. Casciod, F. B. Petersb, K. Hidegc, S. Peukere, P. G. Schultzb and W. L. Hubbe, Site-directed spin labeling of a genetically encoded unnatural amino acid, *Proc. Natl. Acad. Sci. U. S. A.*, 2009, **106**, 21637–21642.
13 P. Kuppusamy, M. Chzhan, K. Vu, M. Shteynbuk, D. J. Lefer, E. Giannella and J. L. Zweier, Three-dimensional spectral-spatial EPR imaging of free radicals in the heart: A technique for imaging tissue metabolism and oxygenation, *Proc. Natl. Acad. Sci. U. S. A.*, 1994, **91**, 3388–3392.
14 A. S. L. Thankamony, J. J. Wittmann, M. Kaushik and B. Corzilius, Dynamic nuclear polarization for sensitivity enhancement in modern solid-state NMR, *Prog. Nucl. Magn. Reson. Spectrosc.*, 2017, **102-103**, 120–195.
15 L. Ji, J. Shi, J. Wei, T. Yu and W. Huang, Air-Stable Organic Radicals: New-Generation Materials for Flexible Electronics?, *Adv. Mater.*, 2020, **32**, 1908015.

16 G.-F. Huo, Q. Tu, X.-L. Zhao, X. Shi and H.-B. Yang, Synthesis and characterization of an unexpected mechanochromicbistricyclic aromatic ene, *Chin. Chem. Lett.*, 2020, **31**, 1847–1850.
17 S. Castellanos, D. Velasco, F. Llpez-Calahorra, E. Brillas and L. Juliá, Taking Advantage of the Radical Character of Tris(2,4,6-trichlorophenyl)methyl To Synthesize New Paramagnetic Glassy Molecular Materials, *J. Org. Chem.*, 2008, **73**, 3759–3767.
18 Q. Peng, A. Obolda, M. Zhang and F. Li, Organic Light-Emitting Diodes Using a Neutral π Radical as Emitter: The Emission from a Doublet, *Angew. Chem., Int. Ed.*, 2015, **54**, 7091–7095.
19 X. Ai, E. W. Evans, S. Dong, A. J. Gillett, H. Guo, Y. Chen, T. J. H. Hele, R. H. Friend and F. Li, Efficient radical-based light-emitting diodes with doublet emission, *Nature*, 2018, **563**, 536–540.
20 Z. Cui, A. Abdurahman, X. Ai and F. Li, Stable Luminescent Radicals and Radical-Based LEDs with Doublet Emission, *CCS Chem.*, 2020, **2**, 1129–1145.
21 S. Kimura, T. Kusamoto, S. Kimura, K. Kato, Y. Teki and H. Nishihara, Magnetoluminescence in a Photostable, Brightly Luminescent Organic Radical in a Rigid Environment, *Angew. Chem., Int. Ed.*, 2018, **57**, 12711–12715.
22 K. Kato, S. Kimura, T. Kusamoto, H. Nishihara and Y. Teki, Luminescent Radical-Excimer: Excited-State Dynamics of Luminescent Radicals in Doped Host Crystals, *Angew. Chem., Int. Ed.*, 2019, **58**, 2606–2611.
23 M. Lucarini, Supramolecular Radical Chemistry, Basic Concepts and Methodologies, in *Encyclopedia of Radicals in Chemistry, Biology and Materials*, Wiley, 2012, vol. 2, p. 229.
24 B. Tang, J. Zhao, J.-F. Xu and X. Zhang, Tuning the stability of organic radicals: from covalent approaches to non-covalent approaches, *Chem. Sci.*, 2020, **11**, 1192–1204.
25 Y. Wang, M. Frasconi and J. F. Stoddart, Introducing Stable Radicals into Molecular Machines, *ACS Cent. Sci.*, 2017, **3**, 927–935.
26 W. S. Jeon, H.-J. Kim, C. Lee and K. Kim, Control of the stoichiometry in host–guest complexation by redox chemistry of guests: Inclusion of methylviologen in cucurbit[8]uril, *Chem. Commun.*, 2002, 1828–1829.
27 A. Y. Ziganshina, Y. H. Ko, W. S. Jeon and K. Kim, Stable π-dimer of a tetrathiafulvalene cation radical encapsulated in the cavity of cucurbit[8]uril, *Chem. Commun.*, 2004, 806–807.
28 A. Trabolsi, N. Khashab, A. C. Fahrenbach, D. C. Friedman, M. T. Colvin, K. K. Cotí, D. Benítez, E. Tkatchouk, J.-C. Olsen, M. E. Belowich, R. Carmielli, H. A. Khatib, W. A. Goddard III, M. R. Wasielewski and J. F. Stoddart, Radically enhanced molecular recognition, *Nat. Chem.*, 2010, **2**, 42–49.
29 B. Tang, W.-L. Li, Y. Chang, B. Yuan, Y. Wu, M.-T. Zhang, J.-F. Xu, J. Li and X. Zhang, A Supramolecular Radical Dimer: High-Efficiency NIR-II Photothermal Conversion and Therapy, *Angew. Chem., Int. Ed.*, 2019, **58**, 15526–15531.
30 D.-W. Zhang, J. Tian, L. Chen, L. Zhang and Z.-T. Li, Dimerization of Conjugated Radical Cations: An Emerging Non-Covalent Interaction for Self-Assembly, *Chem. – Asian J.*, 2015, **10**, 56–68.
31 K. Nakabayashi, Y. Ozaki, M. Kawano and M. Fujita, A Self-Assembled Spin Cage, *Angew. Chem., Int. Ed.*, 2008, **47**, 2046–2048.
32 Y. Ozaki, M. Kawano and M. Fujita, Engineering noncovalent spin–spin interactions in an organic-pillared spin cage, *Chem. Commun.*, 2009, 4245–4247.
33 Y. Ueda, H. Ito, D. Fujita and M. Fujita, Permeable Self-Assembled Molecular Containers for Catalyst Isolation Enabling Two-Step Cascade Reactions, *J. Am. Chem. Soc.*, 2017, **139**, 6090–6093.
34 K. Yazaki, S. Noda, Y. Tanaka, Y. Sei, M. Akita and M. Yoshizawa, An M_2L_4 Molecular Capsule with a Redox Switchable Polyradical Shell, *Angew. Chem., Int. Ed.*, 2016, **55**, 15031–15034.
35 L.-X. Cai, S.-C. Li, D.-N. Yan, L.-P. Zhou, F. Guo and Q.-F. Sun, Water-Soluble Redox-Active Cage Hosting Polyoxometalates for Selective Desulfurization Catalysis, *J. Am. Chem. Soc.*, 2018, **140**, 4869–4876.
36 J. Wang, C. He, P. Wu, J. Wang and C. Duan, An Amide-Containing Metal-Organic Tetrahedron Responding to a Spin-Trapping Reaction in a Fluorescent Enhancement Manner for Biological Imaging of NO in Living Cells, *J. Am. Chem. Soc.*, 2011, **133**, 12402–12405.
37 G.-F. Huo, X. Shi, Q. Tu, Y.-X. Hu, G.-Y. Wu, G.-Q. Yin, X. Li, L. Xu, H.-M. Ding and H.-B. Yang, Radical-Induced Hierarchical Self-Assembly Involving Supramolecular Coordination Complexes in Both Solution and Solid States, *J. Am. Chem. Soc.*, 2019, **141**, 16014–16023.
38 R. Poli, Radical Coordination Chemistry and Its Relevance to Metal-Mediated Radical Polymerization, *Eur. J. Inorg. Chem.*, 2011, 1513–1530.
39 F.-S. Guo, B. M. Day, Y.-C. Chen, M. Tong, A. Mansikkamaki and R. A. Layfield, Magnetic hysteresis up to 80 kelvin in a dysprosium metallocene single-molecule magnet, *Science*, 2018, **362**, 1400–1403.
40 K. Chakarawet, T. D. Harris and J. R. Long, Semiquinone radical-bridged M_2 (M = Fe, Co, Ni) complexes with strong magnetic exchange giving rise to slow magnetic relaxation, *Chem. Sci.*, 2020, **11**, 8196–8203.
41 S. Demir, I.-R. Jeon, J. F. Long and T. D. Harris, Radical ligand-containing single-molecule magnet, *Coord. Chem. Rev.*, 2015, **289–290**, 149–176.
42 Y. Hattori, T. Kusamoto and H. Nishihara, Enhanced Luminescent Properties of an Open-Shell (3,5-Dichloro-4-pyridyl)bis(2,4,6-trichlorophenyl)methyl Radical by Coordination to Gold, *Angew. Chem., Int. Ed.*, 2015, **54**, 3731–3734.
43 Y. Hattori, T. Kusamoto, T. Sato and H. Nishihara, Synergistic luminescence enhancement of a pyridyl-substituted triarylmethyl radical based on fluorine substitution and coordination to gold, *Chem. Commun.*, 2016, **52**, 13393–13396.
44 T. B. Faust and D. M. D'Alessandro, Radicals in metal–organic frameworks, *RSC Adv.*, 2014, **4**, 17498–17512.
45 D. I. Alexandropoulos, B. S. Dolinar, K. R. Vignesh and K. R. Dunbar, Putting a New Spin on Supramolecular

Metallacycles: Co_3 Triangle and Co_4 Square Tetrazine-Based Radicals as Bridges, *J. Am. Chem. Soc.*, 2017, **139**, 11040–11043.

46 W.-L. Jiang, Z. Peng, B. Huang, X.-L. Zhao, D. Sun, X. Shi and H.-B. Yang, TEMPO Radical-Functionalized Supramolecular Coordination Complexes with Controllable Spin–Spin Interactions, *J. Am. Chem. Soc.*, 2021, **143**, 433–441.

47 Y.-F. Han, W.-G. Jia, W.-B. Yu and G.-X. Jin, Stepwise formation of organometallic macrocycles, prisms and boxes from Ir, Rh and Ru-based half-sandwich units, *Chem. Soc. Rev.*, 2009, **38**, 3419–3434.

48 W. Xuan, C. Zhu, Y. Liu and Y. Cui, Mesoporous metal-organic framework materials, *Chem. Soc. Rev.*, 2012, **41**, 1677–1695.

49 X. Han, C. Yuan, B. Hou, L. Liu, H. Li, Y. Liu and Y. Cui, Chiral Covalent Organic Frameworks: Design, Synthesis and Property, *Chem. Soc. Rev.*, 2020, **49**, 6248–6272.

50 R. Chakrabarty, P. S. Mukherjee and P. J. Stang, Supramolecular Coordination: Self-Assembly of Finite Two- and Three-Dimensional Ensembles, *Chem. Rev.*, 2011, **111**, 6810–6918.

51 T. R. Cook, Y.-R. Zheng and P. J. Stang, Metal–Organic Frameworks and Self-Assembled Supramolecular Coordination Complexes: Comparing and Contrasting the Design, Synthesis, and Functionality of Metal–Organic Materials, *Chem. Rev.*, 2013, **113**, 734–777.

52 A. J. McConnell, C. S. Wood, P. P. Neelakandan and J. R. Nitschke, Stimuli-Responsive Metal-Ligand Assemblies, *Chem. Rev.*, 2015, **115**, 7729–7793.

53 L.-J. Chen and H.-B. Yang, Construction of Stimuli-Responsive Functional Materials via Hierarchical Self-Assembly Involving Coordination Interactions, *Acc. Chem. Res.*, 2018, **51**, 2699–2710.

54 M. Pan, K. Wu, J.-H. Zhang and C.-Y. Su, Chiral metal-organic cages/containers (MOCs): from structural and stereochemical design to applications, *Coord. Chem. Rev.*, 2019, **378**, 333–349.

55 M. Pan, W.-M. Liao, S.-Y. Yin, S.-S. Sun and C.-Y. Su, Single-Phase White-Light-Emitting and Photoluminescent Color Tuning Coordination Assemblies, *Chem. Rev.*, 2018, **118**, 8889–8935.

56 H. Cai, Y.-L. Huang and D. Li, Biological metal-organic frameworks: Structures, host–guest chemistry and bio-applications, *Coord. Chem. Rev.*, 2019, **378**, 207–221.

57 H. Zeng, M. Xie, Y.-L. Huang, Y. Zhao, X.-J. Xie, J.-P. Bai, M.-Y. Wan, R. Krishna, W. Lu and D. Li, Induced Fit of C_2H_2 in a Flexible MOF Through Cooperative Action of Open Metal Sites, *Angew. Chem., Int. Ed.*, 2019, **58**, 8515–8519.

58 Z.-Y. Li, Y. Zhang, C.-W. Zhang, L.-J. Chen, C. Wang, H. Tan, Y. Yu, X. Li and H.-B. Yang, Cross-Linked Supramolecular Polymer Gels Constructed from Discrete Multi-pillar[5]arene Metallacycles and Their Multiple Stimuli-Responsive Behavior, *J. Am. Chem. Soc.*, 2014, **136**, 8577–8589.

59 G.-Y. Wu, X. Shi, H. Phan, H. Qu, Y.-X. Hu, X.-L. Zhao, X. Li, L. Xu, Q. Yu and H.-B. Yang, Efficient self-assembly of heterometallic triangular necklace with strong antibacterial activity, *Nat. Commun.*, 2020, **11**, 3178.

60 Y. Hu, W. Wang, R. Yao, X.-Q. Wang, Y.-X. Wang, B. Sun, L.-J. Chen, Y. Zhang, X.-L. Zhao, L. Xu, H.-W. Tan, Y. Yu, X. Li and H.-B. Yang, Facile synthesis of diverse rotaxanes *via* successive supramolecular transformations, *Mater. Chem. Front.*, 2019, **3**, 2397–2402.

61 W. Zheng, G. Yang, S.-T. Jiang, N. Shao, G.-Q. Yin, L. Xu, X. Li, G. Chen and H.-B. Yang, A tetraphenylethylene (TPE)-based supra-amphiphilic organoplatinum(II) metallacycle and its self-assembly behavior, *Mater. Chem. Front.*, 2017, **1**, 1823–1828.

62 X. Ai, Y. Chen, Y. Feng and F. Li, A Stable Room-Temperature Luminescent Biphenylmethyl Radical, *Angew. Chem., Int. Ed.*, 2018, **57**, 2869–2873.

63 S. Shanmugaraju, A. K. Bar, K.-W. Chi and P. S. Mukherjee, Coordination-Driven Self-Assembly of Metallamacrocycles *via* a New Pt^{II}_2 Organometallic Building Block with 90° Geometry and Optical Sensing of Anions, *Organometallics*, 2010, **29**, 2971–2980.

64 S. Shanmugaraju, V. Vajpayee, S. Lee, K.-W. Chi, P. J. Stang and P. S. Mukherjee, Coordination-Driven Self-Assembly of 2D-Metallamacrocycles Using a New Carbazole-Based Dipyridyl Donor: Synthesis, Characterization, and C_{60} Binding Study, *Inorg. Chem.*, 2012, **51**, 4817–4823.

65 S. S. Eaton, K. M. More, B. M. Sawant and G. R. Eaton, Use of the ESR half-field transition to determine the interspin distance and the orientation of the interspin vector in systems with two unpaired electrons, *J. Am. Chem. Soc.*, 1983, **105**, 6560–6567.

66 J. Veciana and I. Ratera, Polychlorotriphenylmethyl Radicals: Towards Multifunctional Molecular Materials. in *Stable Radicals Fundamentals and Applied Aspects of Odd-Electron Compounds*, Wiley, 2010, Chapter 2.

67 R. S. Cahn, S. C. Ingold and V. Prelog, Specification of Molecular Chirality, *Angew. Chem., Int. Ed.*, 1966, **5**, 385–415.

68 M. M. Safont-Sempere, G. Fernandez and F. Wurthner, Self-Sorting Phenomena in Complex Supramolecular Systems, *Chem. Rev.*, 2011, **111**, 5784–5814.

69 P. M. Burrezo, V. G. Jiménez, D. Blasi, I. Ratera, A. G. Campaña and J. Veciana, Organic Free Radicals as Circularly Polarized Luminescence Emitters, *Angew. Chem., Int. Ed.*, 2019, **58**, 16282–16288.

70 Y. Teki, Excited-State Dynamics of Non-Luminescentand Luminescent π-Radicals, *Chem. – Eur. J.*, 2020, **26**, 980–996.

71 X. Yan, T. R. Cook, P. Wang, F. Huang and P. J. Stang, Highly emissive platinum(II) metallacages, *Nat. Chem.*, 2015, **7**, 342–348.

72 F. Fochi, P. Jacopozzi, E. Wegelius, K. Rissanen, P. Cozzini, E. Marastoni, E. Fisicaro, P. Manini, R. Fokkens and E. Dalcanale, Self-Assembly and Anion Encapsulation Properties of Cavitand-Based Coordination Cages, *J. Am. Chem. Soc.*, 2001, **123**, 7539–7552.